Ultra-wide range four-wave mixing in Raman DFB fiber lasers

Jindan Shi*, Shaif-ul Alam, and Morten Ibsen
Optoelectronics Research Centre, University of Southampton, Highfield, Southampton, SO17 1BJ, UK
**Corresponding author: jxs@orc.soton.ac.uk*

We report ultra-wide range and highly efficient wavelength conversion by exploiting four-wave mixing (FWM) in Raman distributed-feedback (R-DFB) fiber lasers. The lasers are 30 cm-long center π phase-shifted DFB gratings UV written in commercially available germano-silica (Ge/Si) single-mode fibers (PS980 from Fibercore Ltd., and UHNA4 from Nufern). The R-DFB lasing signal acts as pump wave for the FWM process within the DFB cavity, and the obtained FWM conversion efficiency is around -25 dB with a maximum wavelength conversion range of 112 nm.

Four-wave mixing (FWM) is a powerful approach to generate radiation at new frequencies through the interaction between light at two or three different incident frequencies, because of (i) the identical features between the converted and the original signals, (ii) the continuous tuning range offered by the process, (iii) transparency in terms of modulation format and, (iv) simultaneous conversion of multiple signals [1-3]. Amongst the nonlinear media for realizing efficient FWM process, optical fiber is uniquely advantageous in the sense that it offers long interaction length within a micron-size core whereby the demand on optical power is largely reduced. In addition, fibers offer low insertion loss when they are integrated into optical transmission systems. Generally speaking, when a strong pump signal and a weak probe signal are injected into a long length (more than a few meters) of a dispersion tailored fiber, a new signal called idler or conjugate wave is generated through the FWM process. When wide conversion range and high conversion efficiency are desired, zero or near-zero dispersion wavelength pumping and a high nonlinear medium are required [4]. These factors pose some limitations to the flexibility of the FWM generation in optical fibers.

A more compact method to obtain FWM would be to use a DFB fiber laser as a mixing device whereby the signal of the DFB laser acts as the pump for the FWM process. This principle was previously reported in the context of semiconductor DFB lasers [3, 5]. However, so far, no FWM-related wavelength conversion has been observed in DFB fiber lasers.

Recently, Raman DFB (R-DFB) fiber lasers with sub-watt level threshold and high output power have been experimentally demonstrated [6, 7]. In that particular design, the phase-shifted DFB grating forms a high reflectivity resonating cavity for the laser signal, whilst being mostly transparent to wavelengths outside the bandgap of the DFB grating. Additionally, it is well-known that the dispersion at the DFB signal wavelength is highly tailored by the DFB grating structure [8]. This opens up the possibility to alleviate the limitation of pumping at or close to the zero-dispersion wavelength of the host fiber by using the DFB signal as the pump for FWM and also helps to eliminate the phase mismatch between the mixing waves.

In this work, we present, for the first time, the demonstration of highly efficient FWM with an ultra-wide wavelength conversion range in two 30 cm-long Raman DFB (R-DFB) fiber lasers formed in different single-mode Ge/Si fibers. The FWM conversion efficiencies (power ratio of the idler to probe waves) are measured to be -25.1 dB and -24.2 dB with the wavelength conversion ranges of 112 nm and 94.1 nm, respectively.

The schematic diagram of the experimental setup is shown in Fig.1. A continuous wave (CW), linearly polarized, Yb-doped polarization maintaining (PM) fiber master oscillator power amplifier at 1064.6 nm (λ_i) is used as the pump source. The output is spliced to a high power isolator and a polarization controller (PC) is used to align the pump polarization state to the R-DFB grating. A 1064nm/1117nm WDM coupler is used to monitor the backward output signal from the system. The forward output is directly coupled into an optical spectrum analyzer (OSA) via a wavelength-independent free-space attenuator (the dotted square box in Fig. 1). All fiber end-facets are angle-cleaved to prevent end-feedback whilst the R-DFB gratings and WDM are mounted on heat sinks to help control the temperature and better remove any generated heat. Note that all the passive components used in this work are non-PM.

Two 30 cm (L1 = 30 cm) long R-DFB gratings, devices reported in the previous works [6, 7], are used for this work. The lasers are written using our continuous grating writing technique that provides unprecedented flexibility when defining the parameters of the grating [9]. One (R-DFB1) is formed in PS980 fiber (from Fibercore Ltd.) with a R-DFB lasing wavelength at 1117.8 nm (λ_{j1}), and the other (R-DFB2) is formed in UHNA4 fiber (from Nufern) with R-DFB lasing wavelength at 1109.7 nm (λ_{j2}). The coupling coefficients are measured to be 37 m^{-1} for R-DFB1 and 30 m^{-1} for R-DFB2 [7], respectively. The numerical aperture, propagation loss (α) @1100 nm and nonlinear coefficient (γ @ the R-DFB signal wavelength) of the two fibers are estimated to be 0.14, 20 dB/km and 6 $(Wkm)^{-1}$ for

PS980, and 0.35, 5 dB/km and 35 $(Wkm)^{-1}$ for UHNA4, respectively. Note that the fiber pigtail at the forward output end of R-DFB gratings is PS980 fiber of a length of L2, as shown in Fig.1.

Fig.2 (a) shows the calculated total group-velocity-dispersion (GVD) of the two fibers whilst the vertical dashed lines indicate the wavelengths of the pump (λ_i), R-DFB signals (λ_{j1} and λ_{j2}) and the corresponding conjugate waves from FWM process at λ_{k1} and λ_{k2}, which satisfy the phase matching condition of: $c/\lambda_{km} = 2\,c/\lambda_{jm} - c/\lambda_i$, where c is the velocity of light in vacuum and m = 1, 2 indicating the lasing wavelengths of R-DFB1 or R-DFB2. It is clearly seen that all operating wavelengths are located in the normal dispersion region of the fibers. However, the dispersive properties at the wavelengths within the bandgap of the DFB gratings are highly tailored by the DFB grating structure [7, 8]. Fig.2 (b) shows the simulated GVD of R-DFB1 grating within the wavelength detuning range of ± 0.02 nm from the center wavelength of 1117.8 nm. As seen, the GVD not only reaches very high values within the ultra-narrow pass-band gap of the grating, but also drops off rapidly inside the pass-band gap centered at the R-DFB wavelength. The GVD inside the bandgap of R-DFB2 grating behaves in a similar manner as illustrated in Fig. 2 (b).

Fig. 3(a) shows the forward output spectra from R-DFB1 with L2 = 1.8 m (trace 1) and L2 = 11.8 m (trace 2) as well as the forward (trace 3) and backward (trace 4) output spectra from R-DFB2 with L2 = 1.8 m at an incident pump power (@1064.6 nm) of 4.1 W. Note that the incident pump power level has been corrected for the insertion loss between the CW pump and the R-DFB device, as seen in Fig.1.

Typical FWM spectra are clearly seen from the forward output spectra (traces 1, 2 and 3), whilst only the R-DFB signal is detected from the backward output (trace 4). This indicates that the FWM originates from the interaction between the pump wave and the co-propagating R-DFB signal. The conjugate waves, as expected, appear at 1176.6 nm (λ_{k1}) from R-DFB1 and 1158.7 nm (λ_{k2}) from R-DFB2, both of which are >40 dB above the noise floor. The frequency shifts between the conjugate waves and the R-DFB signals are 13.4 THz in R-DFB1 and 11.4 THz in R-DFB2, respectively evident that the conjugate waves are indeed generated from the FWM process rather than the second-order Raman Stokes, which should appear at frequencies down-shifted by 13.2 THz from the R-DFB signals. Moreover, we examined the output spectra with two lengths of L2, i.e., 1.8 m and 11.8 m as discussed above, both for R-DFB1 and R-DFB2, and ascertain that the output spectra remain identical with both lengths (traces 1 and 2 in Fig. 3(a) from R-DFB1) of fibers. From these observations we can conclude that the FWM is generated entirely inside the R-DFB fiber laser cavity (with the length of L1 = 30 cm) and not within the pigtail L2 as shown in Fig. 1.

Fig. 3(b) shows the spectra of the pump source (@1064.6 nm) (#1), the R-DFB signals (#2), and the conjugate signals (#3) with the pigtail L2 = 1.8 m at a resolution bandwidth (RBW) of 0.01 nm, measured with an OSA (Advantest Q8384). It is clearly evident that, above the noise floor, the spectra of the conjugate signals (Fig. 3(b) #3) are identical to the spectrum of the CW pump (Fig. 3(b) #1). This is not surprising since the FWM process preserves the phase and amplitude of the wavelength-converted probe signal which in this case is the CW pump (1064.6 nm). The conversion wavelength range between the conjugate wave and the probe signal (1064.6 nm), is 112 nm (corresponding to a frequency shift of 26.8 THz) in R-DFB1 and 94.1 nm (corresponding to a frequency shift of 22.8 THz) in R-DFB2, respectively. This is simply due to the different R-DFB lasing wavelengths of R-DFB1 and R-DFB2.

Fig. 4 shows the FWM conversion efficiencies between the conjugate waves (@ λ_{k1} and λ_{k2}) to the probe wave (λ_i) with respect to the incident CW pump power in R-DFB1 and R-DFB2, respectively. Note that the conversion efficiency is measured from the OSA traces with a RBW of 1 nm. The FWM occurs almost as soon as the threshold for the R-DFB fiber laser is reached [6], and the conversion efficiency increases with increasing CW pump power until the incident pump power reaches ~2.5 W. At this pump-power level, the conversion efficiencies level off at around -25.1 dB and -24.2 dB for R-DFB1 and R-DFB2, respectively. It is worth noting that a comparable conversion efficiency was reported in a 10 km-long single-mode fiber pumped at the zero-dispersion wavelength of the fiber, but in that case the wavelength conversion range was only 7.6 nm [2].

The reasons for such efficient FWM wavelength conversion in a R-DFB fiber laser is believed to be due to the tailoring of the dispersion profile at the R-DFB lasing wavelength resulting from the DFB grating, and the enhancement of intensity of the R-DFB signal at the center of the DFB cavity [10, 11]. Both these factors help in enhancing the nonlinear interaction between CW pump and R-DFB signal to produce the conjugate waves. It is interesting to note that once the R-DFB signal is generated, wavelength conversion of signals other than the DFB laser pump can be achieved as well. We briefly investigated this by conducting a simple experiment whereby the R-DFB devices are concatenated together. Fig. 5 shows the output spectra from the cascaded R-DFB1 and R-DFB2 fiber lasers. In such a case, the R-DFB1 signal not only acts as the pump for FWM in R-DFB1 device, but also serves as the probe wave (probe 2 in Fig. 5) for FWM in R-DFB2 device. Consequently, as seen there are several new wavelengths generated by the FWM process between the CW pump wave and the R-DFB signals. For instance, idlers 1 and 2 are generated through the FWM processes in R-DFB2 from interactions between the pump wave (R-DFB2 signal in this case) and the probes 1 and 2, respectively.

In summary, we have demonstrated for the first time to our knowledge, ultra-compact, highly efficient and ultra-wide range wavelength conversion by using FWM in 30 cm long R-DFB fiber lasers. The lasers were formed in two types of commercially available Ge/Si fibers namely PS980 and UHNA4, respectively. The results from these two lasers are found to be consistent, and the FWM conversion efficiencies are measured to be -25.1 dB (PS980) and -24.2 dB (UHNA4) respectively, when the incident CW pump

power exceeds ~2.5 W, and the corresponding wavelength conversion ranges are found to be 112 nm and 94.1 nm respectively.

References

1. G. P. Agrawal, 2nd Editon (Academic Press) (1995).
2. J. Minch, C. S. Chang, and S. L. Chuang, Photon. Technol. Lett. **4**, 69-72 (1992).
3. J. Minch, C. S. Chang, and S. L. Chuang, Appl. Phys. Lett. **70**, 1360-1362 (1997).
4. A. Camerlingo, F. Parmigiani, F. Xian, F. Poletti, P. Horak, W. H. Loh, D. J. Richardson, and P. Petropoulos, Photon. Technol. Lett. **22**, 628-630 (2010).
5. H. Kuwatsuka, H. Shoji, M. Matsuda, and H. Ishikawa, J. Quantum Elec. **33**, 2002-2010 (1997).
6. J. Shi, S.-u. Alam, and M. Ibsen, Opt. Lett. **37**, 1544-1546 (2012).
7. J. Shi, S.-u. Alam, and M. Ibsen, Opt. Express **20**, 5082-5091 (2012).
8. Z. Qingsheng, in *Antennas and Propagation Society International Symposium,* **1062**, 1060-1063 (*1998)*
9. M. Ibsen, M. K. Durkin, M. J. Cole, and R. I. Laming, Photon. Technol. Lett. **10**, 842-844 (1998).
10. W. H. Loh, B.N. Samson, and J.P.de. Sandro, Appl. Phys. Lett. **69**, 3773-3775 (1996).
11. I. V. Kabakova, T. Walsh, C. M. de Sterke, and B. J. Eggleton, J. Opt. Soc. Am. B **27**, 1343-1351 (2010).

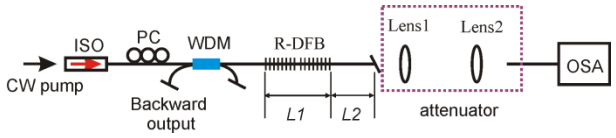

Fig. 1. (Color online) Experimental setup of FWM generation from a R-DFB fiber laser. ISO: isolator; PC: polarization controller; WDM: wavelength division multiplexer; OSA: optical spectrum analyzer.

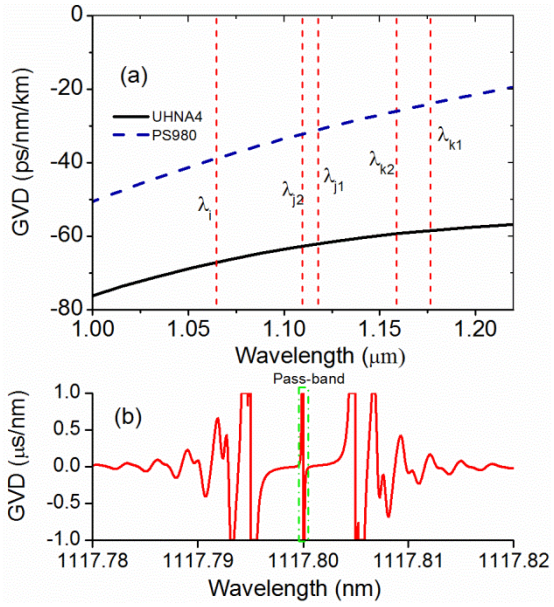

Fig. 2 (Color online) (a) Calculated group-velocity-dispersion (GVD) of the fiber of PS980 and UHNA4, respectively; and (b) calculated GVD of transmitted light of R-DFB1 grating.

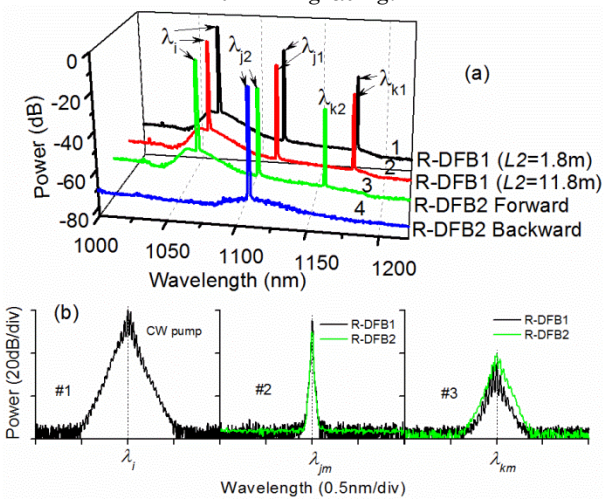

Fig. 3 (Color online) (a): Output spectra from R-DFB1 and R-DFB2 with a RBW of 1 nm. (b): Spectra of CW pump wave (#1), R-DFB signals (#2) and conjugate waves (#3) from R-DFB1 and R-DFB2, respectively at a RBW of 0.01 nm. The vertical dashed lines indicate the wavelengths of CW pump at λ_i (#1), R-DFB signals at λ_{jm} (#2) and conjugate waves at λ_{km} (m=1,2) (#3), respectively.

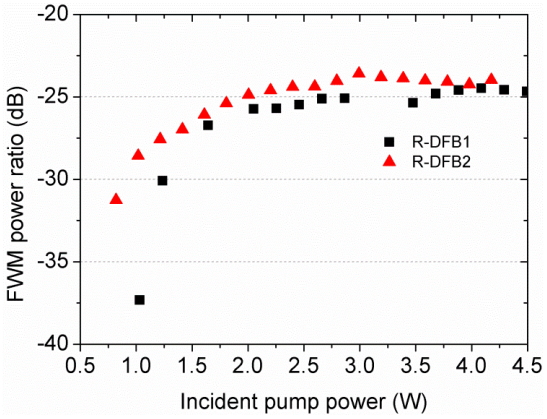

Fig. 4 (Color online) FWM conversion efficiency with respect to the incident CW pump power of 1064.6 nm.

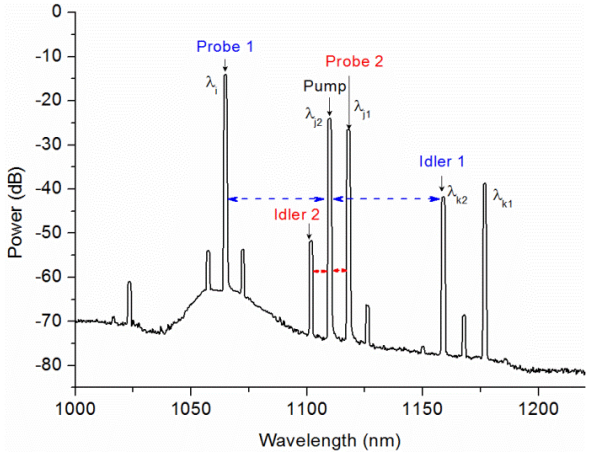

Fig. 5 (Color online) Output spectra from cascaded R-DFB1 and R-DFB2 with a RBW of 1 nm.

1. G. P. Agrawal, "Nonlinear fiber optics," 2nd Editon (Academic Press) (1995).
2. K. Inoue and H. Toba, "Wavelength conversion experiment using fiber four-wave mixing," Photonics Technology Letters, IEEE **4**, 69-72 (1992).
3. J. Minch, C. S. Chang, and S. L. Chuang, "Four-wave mixing in a distributed-feedback laser," Applied Physics Letters **70**, 1360-1362 (1997).
4. A. Camerlingo, F. Parmigiani, F. Xian, F. Poletti, P. Horak, W. H. Loh, D. J. Richardson, and P. Petropoulos, "Wavelength Conversion in a Short Length of a Solid Lead-Silicate Fiber," Photonics Technology Letters, IEEE **22**, 628-630 (2010).
5. H. Kuwatsuka, H. Shoji, M. Matsuda, and H. Ishikawa, "Nondegenerate four-wave mixing in a long-cavity λ/4-shifted DFB laser using its lasing beam as pump beams,"Quantum Electronics, IEEE Journal of **33**, 2002-2010 (1997).
6. J. Shi, S.-u. Alam, and M. Ibsen, "Sub-watt threshold, kilohertz-linewidth Raman distributed-feedback fiber laser," Opt. Lett. **37**, 1544-1546 (2012).
7. J. Shi, S.-u. Alam, and M. Ibsen, "Highly efficient Raman distributed feedback fibre lasers," Opt. Express **20**, 5082-5091 (2012).
8. Z. Qingsheng, "Dispersive properties in phase-shifted Bragg grating filters," in *Antennas and Propagation Society International Symposium, 1998. IEEE*, 1998), 1060-1063 vol.1062.
9. M. Ibsen, M. K. Durkin, M. J. Cole, and R. I. Laming, "Sinc-sampled fibre Bragg gratings for identical multiple wavelength operation," Photonics Technology Letters, IEEE **10**, 842-844 (1998).
10. W. H. Loh, B.N. Samson, and J.P.de. Sandro, "Intensity profile in a distributed feedback fiber laser characterized by a green fluorescence scanning technique," Appl. Phys. Lett., 69(25), 3773-3775 (1996).
11. I. V. Kabakova, T. Walsh, C. M. de Sterke, and B. J. Eggleton, "Performance of field-enhanced optical switching in fiber Bragg gratings," J. Opt. Soc. Am. B **27**, 1343-1351 (2010).